Schloegl's second model for autocatalysis on hypercubic lattices: Dimension dependence of generic two-phase coexistence

Chi-Jen Wang,[1,2] Da-Jiang Liu,[1] and J. W. Evans[1,2,3]
[1]*Ames Laboratory, USDOE, Iowa State University, Ames, Iowa 50011, USA*
[2]*Department of Mathematics, Iowa State University, Ames, Iowa 50011, USA*
[3]*Department of Physics and Astronomy, Iowa State University, Ames, Iowa 50011, USA*
(Received 10 August 2011; published 9 April 2012)

Schloegl's second model on a ($d \geqslant 2$)-dimensional hypercubic lattice involves: (i) spontaneous annihilation of particles with rate p and (ii) autocatalytic creation of particles at vacant sites at a rate proportional to the number of suitable pairs of neighboring particles. This model provides a prototype for nonequilibrium discontinuous phase transitions. However, it also exhibits nontrivial generic two-phase coexistence: Stable populated and vacuum states coexist for a finite range, $p_f(d) < p < p_e(d)$, spanned by the orientation-dependent stationary points for planar interfaces separating these states. Analysis of interface dynamics from kinetic Monte Carlo simulation and from discrete reaction-diffusion equations (dRDEs) obtained from truncation of the exact master equation, reveals that $p_{e(f)} \sim 0.211\ 3765 + c_{e(f)}/d$ as $d \to \infty$, where $\Delta c = c_e - c_f \approx 0.014$. A metastable populated state persists above $p_e(d)$ up to a spinodal $p = p_s(d)$, which has a well-defined limit $p_s(d \to \infty) = \frac{1}{4}$. The dRDEs display artificial propagation failure, absent in the stochastic model due to fluctuations. This feature is amplified for increasing d, thus complicating our analysis.

DOI: 10.1103/PhysRevE.85.041109 PACS number(s): 05.70.Fh, 02.50.Ey, 05.45.−a, 05.50.+q

I. INTRODUCTION

Stochastic lattice-gas reaction and reaction-diffusion models prescribe kinetic rules and rates for the creation and annihilation of various species residing on a lattice [1,2]. The reaction steps are often cooperative and are sometimes irreversible. The lack of a detailed-balance condition on the governing rates means that these systems may evolve to nonequilibrium steady states which are not characterized by a Gibbs measure familiar for thermodynamic equilibrium in Hamiltonian models. However, these steady states can display phase transitions somewhat analogous to those in thermodynamic systems [1,2]. For both equilibrium [3] and nonequilibrium [1] lattice-gas models, it can be instructive to consider behavior as a function of lattice dimension d. For models exhibiting continuous transitions or criticality, an upper critical dimension exists above which fluctuations are weak and mean-field (MF) behavior applies [1,3]. One also expects that either equilibrium or nonequilibrium discontinuous transitions may be erased due to strong fluctuations below some critical $d = d^*$ [1–3].

A candidate for nonequilibrium discontinuous transitions is Schloegl's second model for autocatalysis [4–13] on a hypercubic lattice which involves: (i) spontaneous annihilation of particles X at occupied sites at rate p and (ii) autocatalytic creation of particles at vacant sites ø induced by suitable nearby pairs of particles [8–13]. Schematically, the reaction steps are as follows:

$$X \to \phi \quad \text{(spontaneous annihilation at rate } p\text{)},$$
$$\phi + 2X \to 3X \quad \text{(autocatalytic creation)}.$$

MF analysis suggests the existence of a discontinuous transition between an active state with particle concentration $C > 0$ for $0 < p < p_e$ and an absorbing vacuum state $C = 0$ for all $p > 0$. However, kinetic Monte Carlo (KMC) analysis of Grassberger's version of this model found only a continuous transition for $d < 4$, suggesting a critical $d^* = 4$ [5]. In contrast, our KMC analysis for a version of the model based on Durrett's Quadratic Contact Process (QCP) (see below) revealed a discontinuous transition for $d = 2$ [9] and $d = 3$ [13], suggesting that $d^* = 2$.

In addition, our analysis of the QCP version revealed a *nontrivial* generic two-phase coexistence (2PC) for $d = 2$ and $d = 3$ wherein the stable populated and vacuum phases coexist for a finite range of annihilation rate p [9–13]. (*Trivial* 2PC occurs due to a "quirk" in the QCP rules. For any $p > 0$, the vacuum state can always resist the growth of active droplets which cannot escape any rectangular region containing them [8]. Trivial 2PC disappears upon perturbing the model, e.g., to include particle hopping or spontaneous creation.) The nontrivial 2PC derives from an orientation dependence of the value of the annihilation rate $p = p_{eq}$, corresponding to a stationary planar interface separating the two phases. This nontrivial generic 2PC feature may persist for $d > 3$. This behavior contrasts phase coexistence in an equilibrium Hamiltonian system where planar interface separating phases is stationary at a unique point, corresponding to equality of chemical potentials. As an aside, generic 2PC was explored in Toom's model for voter dynamics [14,15] where the kinetic rules have an unappealing [16] asymmetry.

Our goal here is to elucidate fundamental aspects of the dependence on dimension d of discontinuous transitions in lattice-gas reaction models which display generic 2PC. In this paper, we consider only our QCP version of Schloegl's second model, but the features displayed and issues analyzed will undoubtedly have broad applicability. Analogous studies for equilibrium systems would be performed using the ferromagnetic Ising model. One might expect the kinetics to approach mean-field behavior, and enhanced metastability as $d \to \infty$. However, the d dependence of features related to equistability of distinct phases is perhaps less clear and is the

focus of the current paper. Although contentious [17], we claim that equistability for infinite lattices should be determined by stationarity of planar interfaces separating coexisting states (cf. Refs. [4,18–22]). Consideration of equistability is complicated by the presence of generic 2PC for which we provide an analysis of its d dependence and disappearance as $d \to \infty$.

With regard to development and application of general methodologies, we apply discrete reaction-diffusion equations (dRDEs) to elucidate interface dynamics. dRDEs are derived from truncation approximations to the exact master equations for spatially inhomogeneous states. This approach previously has received little attention, and then only for $d = 1$–3 and mainly using the lowest-order mean-field truncation approximation. We exploit the dRDEs to obtain exact limiting behavior as $d \to \infty$. However, we find that these dRDEs can display artificial propagation failure (APF), an effect which is absent due to fluctuations in the stochastic model and which is strongly amplified with increasing d. Nonetheless, dRDE analysis of suitable interface orientations avoiding APF is shown to still capture behavior in the stochastic model. While we treat only our QCP model, this dRDE methodology and the observed APF behavior and its resolution should have broad applicability.

In Sec. II, we provide a detailed description of our stochastic reaction model for general $d \geqslant 2$. KMC simulation results are reported for $d = 2$–5. In Sec. III, we present the exact master equations for general d and develop dRDEs for spatially heterogeneous states by applying the MF and pair approximations in Sec. IV. The dRDEs are used to assess the propagation of planar interfaces between active and vacuum states, specifically stationarity and APF in Sec. V. The interpretation of the dRDE results and their relationship to exact behavior of the stochastic reaction model is described in Sec. VI. Conclusions are provided in Sec. VII.

II. MODEL PRESCRIPTION FOR GENERAL DIMENSION AND KMC ANALYSIS

Our model involves particle annihilation and creation at the sites of an infinite d-dimensional hypercubic lattice with sites labeled by $\mathbf{i} = (i_1,i_2,i_3,\ldots,i_d)$. Note that the total number of pairs of sites selected from the $2d$ nearest neighbors (NNs) of any site satisfies $k_{\rm tot} = (2d)(2d-1)/2! = d(2d-1)$. We divide all such pairs into two subsets: linear pairs where one site is $(i_1,i_2,\ldots,i_j+1,\ldots,i_d)$ and the other is $(i_1,i_2,\ldots,i_j-1,\ldots,i_d)$ and "diagonal" pairs where one site is at one of $(i_1,i_2,\ldots,i_j\pm1,i_d)$ and another is at one of $(i_1,i_2,\ldots,i_k\pm1,\ldots,i_d)$ and where $j \neq k$. The number of linear pairs satisfies $k_{\rm lin} = d$, and thus, the number of diagonal pairs satisfies $k_{\rm max} = k_{\rm tot} - k_{\rm lin} = 2d(d-1)$. Our QCP version of Schloegl's second model for any $d \geqslant 2$ generalizes Durrett's prescription [8] for a $d = 2$. It involves: (i) spontaneous creation of particles at unoccupied sites at rate p and (ii) autocatalytic annihilation of particles at empty sites at rate $k/k_{\rm max}$, where k is the number of diagonal pairs of particles on neighboring sites. This prescription produces a simple d-independent form for the mean-field kinetics of the model. Furthermore, it enables an exact simplification of the master equations as described in Sec. III.

For spatially homogeneous states, we define the particle concentration C as the mean probability that a site is occupied so that $0 \leqslant C \leqslant 1$. We find that a stable populated steady state with concentration $C > 0$ exists for a range of annihilation rates $0 \leqslant p \leqslant p_e(d)$. Previous KMC papers found $p_e(d=2) = 0.094\ 43$ [9] and $p_e(d=3) = 0.139\ 39$ [13]. Below, we report behavior for $d > 3$. In the "active" populated state, particles are continually created and annihilated. Increasing p to higher $p > p_e(d)$ results in a discontinuous transition to a stable absorbing "vacuum" state with $C = 0$. An ill-defined metastable extension of the active state exists for a small range of $p_e(d) < p < p_s(d)$, where $p_s(d)$ denotes the spinodal with $p_s(d=2) \approx 0.101$ [12] and $p_s(d=3) \approx 0.15$ [13].

Previous papers for $d = 2$ and 3 [9,12] found nontrivial generic 2PC wherein stable active and vacuum states coexist for a finite range $p_f(d) \leqslant p \leqslant p_e(d)$. This range is spanned by the orientation-dependent "equistability" values $p = p_{eq}$ for stationary planar interfaces separating these states, where $p_e(d) = \max p_{eq}$ corresponds to a diagonal ($d = 2$) or skew ($d = 3$) interface. For a general orientation, when $0 \leqslant p < p_{eq}$, the active state displaces the vacuum state. For $p_{eq} < \mathrm{p} < \mathrm{p}_e(d)$, the vacuum state displaces the active state. For $p_e(d) < p < p_s$, the vacuum state transiently displaces the metastable active state until the latter spontaneously converts to the vacuum. One caveat is that, for an exactly vertical interface ($i_1 = 0$), the active state can never propagate into the vacuum (empty sites in this vacuum state have, at most, one occupied neighbor). More precisely, a vertical interface is stationary for all $p \leqslant p_f(d)$, but the vacuum state expands for $p > p_f(d)$. See Refs. [9–13] and Fig. 1. As noted above, trivial 2PC occurs for all $p \leqslant p_e(d)$ as the vacuum state is stable against expansion of droplets of the active state. These features are shown to persist for $d > 3$.

Model behavior is characterized by performing KMC simulations on finite hypercubic lattices of L^d sites with periodic boundary conditions. In conventional constant-p ensemble simulations, processes are implemented with probabilities proportional to their rates. However, to assess p_{eq}, we implement alternative constant-C ensemble simulations [9,23]. System sizes were typically $L = 1024$, 128, 48, and 20, for $d = 2$–5, respectively. Simulation data were collected over times $\sim 10^6$ Monte Carlo steps (MCS) for $d = 2$–4 and $\sim 10^4$ MCS for $d = 5$.

For $d \geqslant 2$ dimensions, the interface orientation where $ai_1 + bi_2 + ci_3 + \cdots = m$ is constant (with a, b, c,..., and m as integers) is labeled by $(abc\cdots)$. Vertical interfaces correspond to $a = 1$ and $b = c = \cdots = 0$ (so $i_1 = m$) are (10), (100), (1000), etc., for $d = 2,3,4,\ldots$, respectively, and have $p_{eq}(d) = p_f(d)$ defined as the upper boundary of the region of propagation failure $0 < p < p_f(d)$. We define a "hyperskew" (HS) orientation as that where $a = b = c = \cdots = 1$ (so $i_1 + i_2 + i_3 + \cdots + i_d = m$) which constitutes the furthest-from-vertical orientation. This hyperskew orientation corresponds to diagonal (11), skew (111), fourth-order skew (1111),..., for $d = 2,3,4,\ldots$, respectively, and has $p_{eq}(d) = p_e(d)$, i.e., p_{eq} is highest for orientations furthest from vertical where the active state can most easily displace the vacuum state. Results for $p_{eq}(d = 2$–$5)$ for various interface

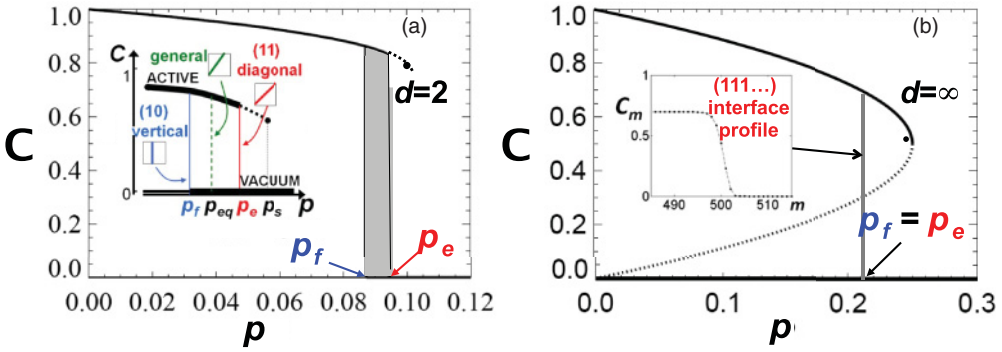

FIG. 1. (Color online) Steady-state C versus p for (a) $d=2$; (b) $d \to \infty$ MF behavior. p_e (p_f) = upper (lower) 2PC boundaries; p_s = spinodal. Inset to (a), dependence of equistability p_{eq} on interface orientation. Inset to (b), profile of a hyperskew interface for $d \to \infty$ at $p_e = p_f = 0.211\,3765$.

orientations are shown in Table I. In Sec. V, we show that $p_{eq}(d \to \infty) = 0.211\,3765$ for all orientations. Our data suggest that $p_{eq}(d) \approx p_{eq}(d \to \infty) + c/d$, where c depends weakly on orientation. See Fig. 2. The width of the 2PC region satisfies $\Delta p_{eq}(d) = p_e(d) - p_f(d) \approx 0.014/d$.

III. MASTER EQUATIONS FOR HOMOGENEOUS AND INHOMOGENEOUS STATES

Let $x(o)$ denote a filled (empty) site, and let P's denote the probabilities for various configurations of clusters of sites. For general spatially inhomogeneous states, the probability that a site is occupied or is vacant depends on its location. Thus, we let $C_{\mathbf{i}} = P[x_{\mathbf{i}}]$ denote the probability that site $\mathbf{i} = (i_1, i_2, \ldots, i_d)$ is occupied. Then, $P[o_{\mathbf{i}}] = 1 - P[x_{\mathbf{i}}]$ is the probability that site $\mathbf{i}$ is empty. Let $\mathbf{e}_1 = (1,0,0,\ldots)$, $\mathbf{e}_2 = (0,1,0,\ldots)$, etc., denote vectors between NN sites. Then, $P[x_{\mathbf{i}}\ \ x_{\mathbf{i}+\mathbf{e}1}]$($P[o_{\mathbf{i}}\ \ o_{\mathbf{i}+\mathbf{e}1}]$) denotes the probability that sites in the NN pair $\mathbf{i}$, $\mathbf{i}+\mathbf{e}_1$ are both occupied (empty). Also, $P[x_{\mathbf{i}}\ \ o_{\mathbf{i}+\mathbf{e}1}]$ and $P[o_{\mathbf{i}}\ \ x_{\mathbf{i}+\mathbf{e}1}]$ denote the probabilities of mixed occupied-empty pairs. Conservation of probability implies that $P[x_{\mathbf{i}}] + P[o_{\mathbf{i}}] = 1$, $P[x_{\mathbf{i}}\ \ o_{\mathbf{i}+\mathbf{e}1}] + P[x_{\mathbf{i}}\ \ x_{\mathbf{i}+\mathbf{e}1}] = P[x_{\mathbf{i}}]$, $P[o_{\mathbf{i}}\ \ x_{\mathbf{i}+\mathbf{e}1}] + P[o_{\mathbf{i}}\ \ o_{\mathbf{i}+\mathbf{e}1}] = P[o_{\mathbf{i}}]$, etc. For the special case of spatially homogeneous states, these quantities do not depend on site location, so $P[x_{\mathbf{i}}] = P[x] = C$, $P[o_{\mathbf{i}}] = P[o] = 1 - C$ ($= C'$), etc. The exact master equations for our reaction model can be written as a coupled hierarchy for the evolution of the probabilities for empty single sites, empty pairs, etc. [24]. Terms in these equations simply account for all possible gain pathways due to spontaneous particle annihilation and all possible loss pathways associated with autocatalytic particle creation.

A. Lowest-order hierarchical equation for single-site probabilities

For spatially inhomogeneous states, the equations for single empty sites have the exact form

$$d/dt\,P[o_{\mathbf{i}}] = pP[x_{\mathbf{i}}] - (1/k_{\max})\{P[o_{\mathbf{i}}\ \ x_{\mathbf{i}+\mathbf{e}1}\ \ x_{\mathbf{i}+\mathbf{e}2}] + P[o_{\mathbf{i}}\ \ x_{\mathbf{i}+\mathbf{e}1}\ \ x_{\mathbf{i}-\mathbf{e}2}] + P[o_{\mathbf{i}}\ \ x_{\mathbf{i}+\mathbf{e}1}\ \ x_{\mathbf{i}+\mathbf{e}3}] + \cdots\} \quad (1)$$

The first gain term on the right-hand side (RHS) of Eq. (1) corresponds to spontaneous particle annihilation at site $\mathbf{i}$ at rate p. The other loss terms correspond to autocatalytic particle creation at empty site $\mathbf{i}$ where one term appears for each of the $k_{\max}$ possible configurations of diagonal pairs of particles on sites NN to $\mathbf{i}$. We have shown explicitly only three out of these $k_{\max}$ creation terms. From Eq. (1), it is clear that, for a spatially homogeneous state, the evolution equation for the probability of a single empty site has the d-independent exact form

$$d/dt\,P[o] = pP[x] - P\left[\begin{matrix} x & \\ o & x \end{matrix}\right]. \quad (2)$$

The loss term on the right-hand side denotes the probability of a filled site with a specific diagonal pair of filled sites, where the state of the $2d-2$ other neighboring sites is unspecified.

In deriving the loss terms in Eq. (1), $P[o_{\mathbf{i}}\ \ x_{\mathbf{i}+\mathbf{e}1}\ \ x_{\mathbf{i}+\mathbf{e}2}]$ corresponds to a sum of contributions for different configurations of the $2d$ sites surrounding $o_{\mathbf{i}}$ but all including a diagonal pair of particles at sites $\mathbf{i}+\mathbf{e}_1$ and $\mathbf{i}+\mathbf{e}_2$. One case is the configuration with all other $2d-2$ neighboring sites empty, so $k=1$, associated with a creation rate of $1/k_{\max}$. The general case has $k-1$ additional diagonal pairs with creation rate $k/k_{\max}$. We associate a fraction $1/k$ of this contribution with the term $P[o_{\mathbf{i}}\ \ x_{\mathbf{i}+\mathbf{e}1}\ \ x_{\mathbf{i}+\mathbf{e}2}]$, and the rest is equally distributed between the other terms. Summing all

TABLE I. KMC values of $p = p_{eq}$ for stationary planar interfaces separating populated and vacuum states for orientations indicated before the colon; $p_{eq} \to 0.211\,377$ as $d \to \infty$ for all orientations.

$d=2$	10:0.0871	11:0.094 40 (2)			
$d=3$	100:0.1353	110:0.139 027(7)	111:0.139 386(7)		
$d=4$	1000:0.1548	1100:0.157 593(9)	1110:0.158 091(8)	1111:0.158 284(8)	
$d=5$	10 000:0.1664	11 000:0.168 24(1)	11 100:0.168 847(7)	11 110:0.169 055(6)	11 111:0.169 137(6)

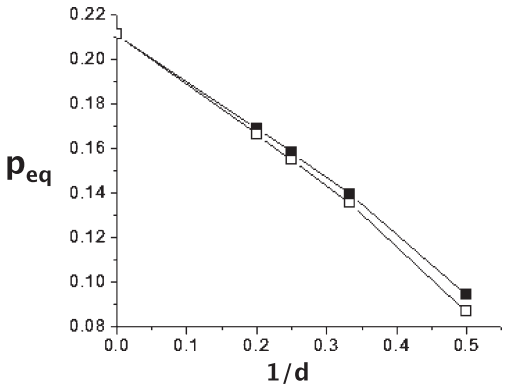

FIG. 2. KMC results for p_{eq} versus $1/d$ for hyperskew (filled square) and vertical (open square) interfaces where the exact result is also shown for $d \to \infty$.

contributions associated with $P[o_{\mathbf{i}}\ x_{\mathbf{i}+\mathbf{e}1}\ x_{\mathbf{i}+\mathbf{e}2}]$, thus, yields $1/k_{\max}$ times the probability that site $\mathbf{i}$ is empty, and the indicated diagonal pair is occupied (with all other neighbors of the empty site in an unspecified state). A similar analysis generates $P[o_{\mathbf{i}}\ x_{\mathbf{i}+\mathbf{e}1}\ x_{\mathbf{i}-\mathbf{e}2}]$ and the other terms.

For spatially inhomogeneous states corresponding to planar interfaces between populated and vacuum states, Eq. (1) adopts a simpler form. For specific orientations, the $C_{i1,i2,\ldots,id}$ and related probabilities can be independent of some i_k or dependent only on certain combinations of them. Also, some probabilities for configurations of clusters of sites become identical. For example, for vertical interfaces where $C_{i1,i2,\ldots,id} = C_{i1}$, the first two particle creation terms in Eq. (1) are equivalent.

B. Hierarchical equation for pair probabilities

One can also obtain equations for probabilities of adjacent empty pairs of sites and for larger clusters of empty sites. For a spatially inhomogeneous state, the evolution equation for the pair probability $P[o_{\mathbf{i}}\ o_{\mathbf{i}+\mathbf{e}1}]$ has the exact form

$$\begin{aligned} d/dt\, P[o_{\mathbf{i}}\, o_{\mathbf{i}+\mathbf{e}1}] &= p\{P[x_{\mathbf{i}}\, o_{\mathbf{i}+\mathbf{e}1}] + P[o_{\mathbf{i}}\, x_{\mathbf{i}+\mathbf{e}1}]\} - (1/k_{\max}) \\ &\quad \times \{P[o_{\mathbf{i}}\, o_{\mathbf{i}+\mathbf{e}1} x_{\mathbf{i}+2\mathbf{e}1} x_{\mathbf{i}+\mathbf{e}1+\mathbf{e}2}] + \cdots\} \\ &\quad - (1/k_{\max})\{P[x_{\mathbf{i}+\mathbf{e}2}\, x_{\mathbf{i}-\mathbf{e}1}\, o_{\mathbf{i}}\, o_{\mathbf{i}+\mathbf{e}1}] + \cdots\}. \end{aligned} \tag{3}$$

The first two gain terms on the RHS correspond to spontaneous particle annihilation at site $\mathbf{i}$ and $\mathbf{i} + \mathbf{e}_1$ at rate p. The next group of loss terms corresponds to autocatalytic particle creation at empty site $\mathbf{i} + \mathbf{e}_1$ where one term appears for each of the $2(d-1)$ possible configurations of diagonal pairs of particle NNs for this site, where neither particle is on the neighboring site $\mathbf{i}$. We have shown explicitly only one out of the subset of $2(d-1)$ configurations where one particle forms a linear triple with the empty pair. There is another larger subset of $2(d-1)(d-2)$ configurations where neither particle forms a linear triple with the empty pair. The analogous last group of loss terms corresponds to autocatalytic particle creation at empty site $\mathbf{i}$ where one term appears for each of the total of $2(d-1)^2$ possible configurations of diagonal pairs of particle NNs for this site.

From Eq. (3), it follows that, for a spatially homogeneous state, the equation for evolution of the probability of an empty pair has the exact form

$$\begin{aligned} d/dt\, P[o\ o] &= 2pP[x\ o] - \{4(d-1)/k_{\max}\}P\begin{bmatrix} & x & \\ o & o & x \end{bmatrix} \\ &\quad - \{4(d-1)(d-2)/k_{\max}\}P\begin{bmatrix} & x & \\ o & \otimes & \end{bmatrix}, \end{aligned} \tag{4}$$

where $P\left[\begin{smallmatrix} & x & \\ o & o & x \end{smallmatrix}\right]$ and $P\left[\begin{smallmatrix} & x & \\ o & \otimes & \end{smallmatrix}\right]$ represent probabilities of an empty pair where the right site in this pair has a diagonal neighboring pair of particles. In the first, one filled site forms a linear triple with the empty pair. In the second, both filled sites form bent triples with the empty pair.

Derivation of the loss terms in Eq. (3) due to autocatalytic particle creation follows a similar strategy as that for Eq. (1) above. Each term corresponds to a sum of contributions associated with different configurations of the $2d-1$ sites at the relevant end of the empty pair $[o_{\mathbf{i}}\ o_{\mathbf{i}+\mathbf{e}1}]$ but which all include the diagonal pair of particles indicated explicitly in Eq. (3). Summing all contributions associated with the specific pair, thus, yields $1/k_{\max}$ times the probability that the pair is empty, and the specific diagonal pair is occupied (with other neighbors of the empty pair unspecified).

IV. APPROXIMATIONS AND DISCRETE REACTION-DIFFUSION EQUATIONS

A. Truncation approximations

In the simplest MF or site approximation, one neglects all correlations in the occupancy of different sites. Thus, for example, one has that

$$\begin{aligned} &P[o_{\mathbf{i}}\ x_{\mathbf{i}+\mathbf{e}1}\ x_{\mathbf{i}+\mathbf{e}2}] \\ &\quad \approx P[o_{\mathbf{i}}]P[x_{\mathbf{i}+\mathbf{e}1}]P[x_{\mathbf{i}+\mathbf{e}2}] \\ &\qquad \left(\text{reducing to } P\begin{bmatrix} x & \\ o & x \end{bmatrix} \approx P[o]P[x]^2\right) \end{aligned} \tag{5}$$

for inhomogeneous (homogeneous) states. In the next higher-order pair approximation, probability configurations of clusters of sites are factorized in terms of those for all constituent pairs where one also compensates for double counting of some sites. Thus, one has that

$$\begin{aligned} &P[o_{\mathbf{i}}\, x_{\mathbf{i}+\mathbf{e}1}\, x_{\mathbf{i}+\mathbf{e}2}] \approx P[o_{\mathbf{i}}\, x_{\mathbf{i}+\mathbf{e}1}]P[o_{\mathbf{i}}\, x_{\mathbf{i}+\mathbf{e}2}]/P[o_{\mathbf{i}}] \\ \text{and}\quad &P[o_{\mathbf{i}} o_{\mathbf{i}+\mathbf{e}1}\, x_{\mathbf{i}+2\mathbf{e}1}\, x_{\mathbf{i}+\mathbf{e}1+\mathbf{e}2}] \\ &\quad \approx P[o_{\mathbf{i}} o_{\mathbf{i}+\mathbf{e}1}]P[o_{\mathbf{i}+\mathbf{e}1}\, x_{\mathbf{i}+2\mathbf{e}1}] \\ &\qquad \times P[o_{\mathbf{i}+\mathbf{e}1}\, x_{\mathbf{i}+\mathbf{e}1+\mathbf{e}2}]/P[o_{\mathbf{i}+\mathbf{e}1}]^2 \end{aligned} \tag{6}$$

(reducing to $P\left[\begin{smallmatrix} x & \\ o & x \end{smallmatrix}\right] \approx P[x\ o]^2/P[o]$ and $P\left[\begin{smallmatrix} & x & \\ o & o & x \end{smallmatrix}\right] \approx P\left[\begin{smallmatrix} & x & \\ o & \otimes & \end{smallmatrix}\right] \approx P[o\ o]P[x\ o]^2/P[o]^2$), for inhomogeneous (homogenous) states.

B. Mean-field type kinetics for homogeneous states

The MF site approximation for Eq. (2) yields the d-independent MF kinetics,

$$\begin{aligned} &d/dt\ C = -pC + C^2(1-C) \equiv R(C), \\ &\text{so } d/dt\ \ln C' = (C/C')[p - CC'], \end{aligned} \tag{7}$$

where $C' = 1 - C$ gives the probability of an empty site. Steady-state analysis reveals a stable vacuum state with $C = 0$ for all $p > 0$ and a stable active state with $C = C_{act}(\mathrm{MF}) = \frac{1}{2} + \frac{1}{2}(1-4p)^{1/2}$ for a bistability regime $0 \leqslant p \leqslant p_s(\mathrm{MF}) = \frac{1}{4}$ [4,8–10]. In the pair approximation, a natural variable is the conditional concentration, $K = P[x\ o]/P[o]$, representing the probability of finding a particle next to a site specified empty. Setting $K' = 1 - K$ (the conditional probability of an empty site) and $c_d = (d-1)/d$, the pair kinetics can be instructively formulated as

$$d/dt \ln C' = (C/C')[p - CC'(K/C)^2]$$
$$\text{and} \quad d/dt \ln K' + d/dt \ln C' = 2(K/K')[p - c_d K K']. \tag{8}$$

A steady-state analysis yields a stable vacuum state with $C = K = 0$ for all $p > 0$, and a stable active state $K = K_{\mathrm{act}}(\mathrm{pair}) = \frac{1}{2} + \frac{1}{2}(1-4p/c_d)^{1/2}$ for a bistability regime $0 \leqslant p \leqslant p_s(\mathrm{pair}) = c_d/4$. Since $c_d \to 1$ as $d \to \infty$, it is clear comparing Eqs. (7) and (8) that site and pair approximations converge.

More generally, consider the evolution of the probability $P[\{o\}_n]$ of a finite connected cluster of n vacant sites $\{o\}_n$. The key observation is that, as $d \to \infty$, all sites are on the perimeter and almost fully coordinated with sites not in the cluster. More precisely, the fractional deficit from full coordination scales, such as $1/d$. Thus, the structure of the evolution equation is similar to that for the probability $(P[o])^n$ for n isolated far-separated sites. It follows that $P[\{o\}_n] \to (P[o])^n$ as $d \to \infty$, a general feature, applying for any lattice-gas reaction model.

C. Mean-field-type dRDE

We will consider only spatially inhomogeneous states corresponding to planar interfaces between active and vacuum states. As in Sec. II, interface orientations where $ai_1 + bi_2 + ci_3 + \cdots = m$ is constant are labeled by $(abc\cdots)$ for $d \geqslant 2$ dimensions. In these cases, the concentrations $C_{i1,i2,\ldots,id} = C_{ai1+bi2+ci3\cdots=m} = C_m$ are labeled by a single integer m. Applying MF factorization to Eq. (1) produces dRDE-type equations for the C_m. The "diffusion"-type terms reflect spatial coupling in the reaction model rather than particle hopping. These types of MF dRDEs have been explored previously for other reaction-diffusion models, but only for $d \leqslant 3$ [25–27]. It is convenient to define a pseudodiffusion coefficient $D_j(C) = C(1-C)/j$ and the discrete Laplacian,

$$\Delta C_m = C_{m+1} - 2C_m + C_{m-1} \quad \text{so that}$$
$$(C_{m+1} + C_{m-1})^2 - (2C_m)^2 = 4C_m \Delta C_m + (\Delta C_m)^2. \tag{9}$$

For hyperskew $(1111\cdots)$ interfaces where $C_{i1,i2,\ldots,id} = C_{i1+i2+\cdots+id=m}$, one obtains the MF dRDEs,

$$\begin{aligned} d/dt\ C_m &= -pC_m + \tfrac{1}{4}(1-C_m)(C_{m+1} + C_{m-1})^2 \\ &= R(C_m) + D_1(C_m)\Delta C_m \\ &\quad + \tfrac{1}{4}(1-C_m)(C_{m+1} + C_{m-1})^2, \end{aligned} \tag{10}$$

which have a form independent of d. As a consequence, the MF value of p_{eq} for the $d = 2$ diagonal, $d = 3$ skew, and $d > 3$ hyperskew orientations will be identical. It should be noted that the physical Euclidean distance between adjacent planes m and $m+1$ equals $d^{-1/2}$, and thus, the physical width of the concentration profile across the interface also scales like $d^{-1/2}$.

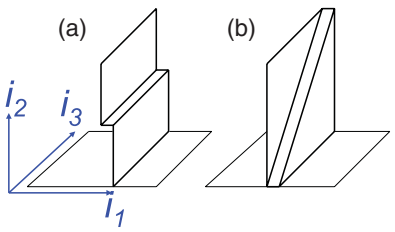

FIG. 3. (Color online) Schematic for $d = 3$ of (a) a rare horizontal and (b) a hyperskew step on a vertical interface.

For vertical $(1000\cdots)$ interfaces where $C_{i1,i2,\ldots,id} = C_{i1=m}$, one obtains the distinct MF dRDE,

$$d/dtC_m = R(C_m) + D_d(C_m)\Delta C_m, \tag{11}$$

incorporating weak spatial coupling for large d due to small $D_d \sim 1/d$. Since $R(0) = 0$ and $D_d(0) = 0$, Eq. (11) appropriately ensures that the active state cannot displace the vacuum state.

Next, consider more general low-index interfaces including diagonal $(11\,000\cdots)$ interfaces where $C_{i1,i2,\ldots,id} = C_{i1+i2=m}$, skew $(11\,100\cdots)$ interfaces $C_{i1,i2,\ldots,id} = C_{i1+i2+i3=m}$, and the natural generalization to nth-order skew interfaces where $C_{i1,i2,\ldots,id} = C_{i1+i2+i3+\cdots+in=m}$. For the general nth-order skew case, one obtains the MF RDE,

$$\begin{aligned} d/dtC_m &= R(C_m) + nD_d(C_m)\Delta C_m \\ &\quad + \tfrac{1}{4}n(n-1)d^{-1}(d-1)^{-1}(\Delta C_m)^2. \end{aligned} \tag{12}$$

This result includes vertical $(n = 1)$, diagonal $(n = 2)$, and skew $(n = 3)$ orientations as special cases and reveals weak spatial coupling in all cases with $n = O(1)$ and large d in contrast to Eq. (10).

For reasons discussed below, it will also be instructive to consider near-vertical orientations. When $Si_1 + i_2 = m$, corresponding to a near-vertical interface with large slope S and far-spaced rare "horizontal steps" [see Fig. 3(a)], one obtains the MF dRDE,

$$\begin{aligned} d/dtC_m &= -pC_m + d^{-1}(d-1)^{-1}(d-2)(d-3) \\ &\quad \times (1-C_m)(C_m)^2 + d^{-1}(d-1)^{-1}(d-2)(1-C_m) \\ &\quad \times C_m(C_{m-1} + C_{m+1} + C_{m-S} + C_{m+S}) \\ &\quad + \tfrac{1}{2}d^{-1}(d-1)^{-1}(1-C_m)(C_{m-1} + C_{m+1}) \\ &\quad \times (C_{m-S} + C_{m+S}). \end{aligned} \tag{13}$$

When $Si_1 + i_2 + \cdots + i_d = m$, corresponding to a near-vertical interface with large slope S and far-spaced rare "maximally kinked" or hyperskew steps [see Fig. 3(b)], one obtains the MF dRDE,

$$\begin{aligned} d/dtC_m &= -pC_m + \tfrac{1}{4}d^{-1}(d-2)(1-C_m)(C_{m-1} + C_{m+1})^2 \\ &\quad + \tfrac{1}{2}d^{-1}(1-C_m)(C_{m-1} + C_{m+1})(C_{m-S} + C_{m+S}). \end{aligned} \tag{14}$$

Writing Eqs. (13) and (14) in the form $d/dtC_m = R(C_m) +$ "diffusion-type terms," these diffusion terms are on the order of $1/d$ in Eq. (13) but on the order of unity in Eq. (14) [which reduces to Eq. (10) as $d \to \infty$].

One can also apply the pair approximation to Eqs. (1) and (3) for planar interfaces between active and vacuum states to

TABLE II. MF results for stationary points $p = p_{eq}$ for regimes of propagation failure for planar interfaces separating populated and vacuum states. Results shown for $S = 1024$.

	Vertical $1000\cdots$	$Si_1 + i_2$	$Si_1 + i_2 + \cdots + i_d$	Diagonal $11\,000\cdots$	$S(i_1 + i_2) + i_3 + \cdots + i_d$	Skew $11\,100\cdots$	$S(i_1 + i_2 + i_3) + i_4 + \cdots + i_d$	Hyperskew $111\cdots$
$d=2$	0.207 1068	0.205 051						0.211 3765
$d=3$	0.210 38	0.206 02	0.206 05	0.210 23–0.210 37	0.210 30			0.211 3765
$d=4$	0.215 14	0.207 20	0.207 32	0.209 49–0.210 27	0.209 90	0.210 93	0.210 92	0.211 3765
$d=5$	0.219 53	0.207 82–0.208 29	0.208 34	0.208 20–0.210 99	0.209 74	0.210 60–0.210 75	0.210 68	0.211 3765
$d=6$	0.223 12	0.207 17–0.209 74	0.209 06	0.205 83–0.212 46	0.209 71	0.210 24–0.210 81	0.210 53	0.211 3765
$d=7$	0.226 00	0.204 68–0.211 75	0.209 57	0.202 22–0.214 37	0.209 77	0.209 59–0.211 20	0.210 45	0.211 3765
$d=10$	0.231 88	0.188 16–0.218 45	0.210 39	0.185 59–0.220 35	0.210 15	0.204 96–0.214 14	0.210 39	0.211 3765
$d=100$	0.247 73	0.032 35–0.245 58	0.211 365	0.032 34–0.245 66	0.211 35	0.049 77–0.243 70	0.211 34	0.211 3765
$d=1000$	0.249 76	0.003 39–0.249 52	0.211 3764	0.003 40–0.249 52	0.211 3763	0.005 31–0.249 29	0.211 3762	0.211 3765
$d=\infty$	0–0.25	0–0.25		0–0.25		0–0.25		0.211 3765

obtain pair dRDEs for C_m and related pair probabilities. See Appendix A for the special cases of hyperskew $(1111\cdots)$ and vertical $(1000\cdots)$ interfaces.

V. dRDE ANALYSIS: MEAN-FIELD AND PAIR RESULTS

We now present results from numerical integration of the dRDEs for evolution of planar interfaces between the active and the vacuum states. The initial data are chosen as a sharp interface between the active state $C_m = C_{\text{act}}$ for $m < m^*$ and the vacuum state $C_m = 0$ for $m \geqslant m^*$. In the pair approximation, we also specify certain pair occupations determined from $K_{\text{act}}(\text{pair})$. The interface location is determined from $\langle m \rangle = \sum_m C_m / C_{\text{act}}$ for a large finite system of $\sim$1000 sites. The interface velocity $V(p) = d/dt\,\langle m \rangle$ is determined for long times $t \approx 4 \times 10^4$. Our focus is on assessing variation in $V(p)$ with p to determine stationarity and propagation failure.

A. Hyperskew $(1111\cdots)$ orientation

The MF dRDEs for the hyperskew orientation where $m = i_1 + i_2 + \cdots + i_d$ have the special feature of being independent of d. Analysis of interface propagation reveals that $V(p)$ vanishes at a single stationary point which has the d-independent MF value $p_{eq}(111\cdots) = 0.211\ 3765(4)$. See Table II. The pair dRDEs for the hyperskew orientation predict qualitatively similar interface evolution with $V(p)$ vanishing at a single stationary point. However, the pair $p_{eq}(111\cdots)$ depends on dimension and increases smoothly to converge to the MF value as $d \to \infty$. See Table III. Continuously deviating from a hyperskew orientation produces continuous deviations from the above behavior either at the MF or at the pair level with p_{eq} shifting to lower values.

B. Vertical $(1000\cdots)$ and near-vertical orientations

The MF dRDEs for vertical interfaces where $m = i_1$ predict propagation failure for $0 < p < p_{eq}(100\cdots)$ where MF $p_{eq}(100\cdots)$ increases with d. In fact, MF $p_{eq}(100\cdots) \to p_s(\text{MF}) = \frac{1}{4}$ as $d \to \infty$ where the interface is stationary over the entire bistability regime. See Table II. Additional analysis elucidates the sharpening of the stationary interface at $p = p_{eq}$ as d increases. See Appendix B. Analysis of the pair dRDEs, Eq. (A1), reveals the same qualitative behavior where the pair $p_{eq}(100\cdots) \to p_s(\text{MF}) = \frac{1}{4}$ as $d \to \infty$ but the rate of convergence is slower. See Table III.

1. Deviation from a vertical orientation with rare horizontal "steps" [cf. Fig. 3(a)]

Both MF and pair analysis for near-vertical orientations with rare horizontal (H) steps $(Si_1 + i_2 = m$ with large $S = 1024)$ indicates a unique stationary point $p_{eq}(100\cdots H)$ for $d = 2$–5, which shifts upward with d. For $d \geqslant 6$, a finite range of propagation failure emerges over a

TABLE III. Pair approximation results for stationary points $p = p_{eq}$ or for regimes of propagation failure for planar interfaces separating populated and vacuum states. Results shown for $S = 1024$.

	Vertical $100\cdots$	$Si_1 + i_2$	$Si_1 + i_2 + \cdots + i_d$	Diagonal $11\,000\cdots$	$S(i_1 + i_2) + i_3 + \cdots + i_d$	Skew $11\,100\cdots$	$S(i_1 + i_2 + i_3) + i_4 + \cdots + i_d$	Hyperskew $111\cdots$
$d=2$	0.106 016	0.105 596		0.108 312				0.108 312
$d=3$	0.141 23	0.139 89	0.139 89	0.142 51	0.142 51			0.142 95
$d=4$	0.160 84	0.157 14	0.157 16	0.159 30–0.159 41	0.159 36	0.159 90	0.159 90	0.160 14
$d=5$	0.174 71	0.167 83–0.167 86	0.167 94	0.169 02–0.169 72	0.169 39	0.170 02	0.170 01	0.170 42
$d=6$	0.185 00	0.174 76–0.175 33	0.175 27	0.174 60–0.177 26	0.176 08	0.176 64–0.176 77	0.176 71	0.177 26
$d=7$	0.192 88	0.178 60–0.181 38	0.180 55	0.177 13–0.183 49	0.180 90	0.181 20–0.181 75	0.181 49	0.182 15
$d=10$	0.208 14	0.174 46–0.195 93	0.190 03	0.172 04–0.197 69	0.189 85	0.186 83–0.192 56	0.190 12	0.190 93
$d=100$	0.245 25	0.032 19–0.243 10	0.209 32	0.032 18–0.243 18	0.209 31	0.049 52–0.241 24	0.209 30	0.209 33
$d=1000$	0.249 51	0.003 39–0.249 27	0.211 17	0.003 39–0.249 27	0.211 17	0.005 39–0.249 04	0.211 17	0.211 17
$d=\infty$	0–0.25	0–0.25		0–0.25		0–0.25		0.211 3765

regime $p_-(100\cdots H) < p < p_+(100\cdots H)$. This regime expands with increasing d to cover the entire region of bistability, i.e., $p_-(100\cdots H) \to 0$ and $p_+(100\cdots H) \to p_s(\mathrm{MF}) = \frac{1}{4}$ as $d \to \infty$. See Tables II and III.

2. *Deviation from a vertical orientation with rare HS steps [cf. Fig. 3(b)]*

Orientations defined by $Si_1 + i_2 + \cdots + i_d = m$ with large S correspond to a vertical interface $i_1 = 0$ misoriented by occasional hyperskew (maximally kinked) steps separated by vertical S lattice constants. Analysis based on both the MF and the pair dRDEs for $S = 1024$ indicates a unique stationary point for which $p_{eq}(100\cdots HS) \to \lim_{d\to\infty} p_{eq}(111\cdots) = 0.211\ 3765$, as $d \to \infty$. See Tables II and III.

C. Diagonal (11 000 · · ·), skew(11 100 · · ·), and other orientations

Analysis of the MF and pair dRDEs for diagonal $(11\ 000\cdots)$ interfaces where $m = i_1 + i_2$ reveals that, except for small d, one has propagation failure over a regime $p_-(1100\cdots) < p < p_+(1100\cdots)$. The regime of propagation failure expands with increasing d to cover the entire region of bistability, i.e., $p_-(1100\cdots) \to 0$ and $p_+(1100\cdots) \to p_s(\mathrm{MF}) = \frac{1}{4}$ as $d \to \infty$. See Tables II and III. Motivated by the analysis of near-vertical interfaces, we also consider deviations from diagonal orientations associated with rare hyperskew (maximally kinked) steps as a route to eliminate propagation failure. These orientations are described by $S(i_1 + i_2) + i_3 + i_4 + \cdots + i_d = m$, where we choose $S = 1024$. Analysis for the MF and pair dRDEs reveals a lack of propagation failure with stationary point $p_{eq}(1100\cdots HS) \to \lim_{d\to\infty} p_{eq}(111\cdots) = 0.211\ 3765$ as $d \to \infty$. See Tables II and III.

Analysis of both MF and pair dRDEs for skew $(11\ 100\cdots)$ interfaces reveals that, except for small d, one has propagation failure over a regime $p_-(1110\cdots) < p < p_+(1110\cdots)$. Again, the regime of propagation failure expands with increasing d to cover the entire region of bistability, i.e., $p_-(1110\cdots) \to 0$ and $p_+(1110\cdots) \to p_s(\mathrm{MF}) = \frac{1}{4}$ as $d \to \infty$. It is also the case that propagation failure can be eliminated by deviating from skew orientations with rare hyperskew steps. These orientations are described by $S(i_1 + i_2 + i_3) + i_4 + \cdots + i_d = m$ where we choose $S = 1024$. The stationary point $p_{eq}(1110\cdots HS) \to \lim_{d\to\infty} p_{eq}(111\cdots) = 0.211\ 3765$ as $d \to \infty$. See Tables II and III.

One can extend the above investigations to consider nth-order skew orientations as defined in Sec. IV B. One anticipates analogous behavior, i.e., development of propagation failure with increasing d, which engulfs the entire bistable regime as $d \to \infty$. It is also anticipated that deviating from these orientations with rare hyperskew steps eliminates propagation failure.

VI. RELATING dRDE PREDICTIONS TO STOCHASTIC MODEL BEHAVIOR

In relating MF-type dRDE predictions to stochastic reaction model behavior, it is instructive to first focus on two key interface orientations, hyperskew and vertical.

For hyperskew $(111\cdots)$ interfaces, the correspondence is unambiguous: There is no propagation failure for MF or pair dRDEs, and the predicted $p_{eq}(111\cdots)$ corresponds to that in the stochastic model. The large discrepancy between the d-independent MF predictions and the KMC values of $p_{eq}(111\cdots)$ for smaller d is largely removed in the pair approximation. As noted previously, the simple form $p_{eq}(111\cdots) \approx 0.211\ 3765 + c/d$ describes well observed d dependence.

For vertical $(100\cdots)$ interfaces, recall that propagation failure is expected for p below some critical value, $p_{eq}(1000\cdots)$ as the active state cannot displace the vacuum state for any $p \geqslant 0$. For $p > p_{eq}(1000\cdots)$, the vacuum state displaces the populated state. This feature applies to both the stochastic model and to the various MF-type dRDEs. However, $p_{eq}(1000\cdots)$, from MF-type treatments, does not correspond to that for the stochastic model as estimated by KMC simulations. Specifically, MF-type formulations "artificially extend" the regime of propagation failure. This feature is amplified for increasing d, recalling that MF-type $p_{eq}(1000\cdots) \to p_s(\mathrm{MF}) = \frac{1}{4}$ as $d \to \infty$.

Artificial propagation failure (APF) in MF-type dRDE treatments can be understood as follows. For smooth vertical interfaces in the stochastic lattice-gas reaction model, propagation of the vacuum state into the populated state for $p > p_{eq}$ is associated with fluctuation-mediated nucleation and growth of $(d-1)$-dimensional droplets of the vacuum state in the layer adjacent to the completely empty edge layer of the vacuum state. This feature is not reflected in MF-type treatments where more difficult "spatially homogeneous propagation" of the vacuum state into the next layer is required.

Considering near-vertical interfaces in MF-type treatments, i.e., vertical interfaces with far-separated steps, could potentially avoid APF. However, introducing "smooth" horizontal steps does not avoid APF. Why? Step propagation in the MF dRDE must occur by spatially homogeneous propagation rather than by fluctuation-mediated nucleation and growth of new rows of empty sites adjacent to the step as in the stochastic reaction model. However, introducing more easily propagating maximally kinked hyperskew steps avoids APF.

The amplification of APF with increasing d follows from the form of the MF-type dRDEs. For vertical interfaces, the spatial coupling in MF-type dRDEs is $\sim 1/d$ [cf. Eq. (11)]. The diminution of this coupling with increasing d produces an amplification of APF. The same diminution of coupling persists upon introducing rare horizontal steps to a vertical interface [cf. Eq. (13)], thus, preserving APF. However, introduction of rare hyperskew steps results in strong spatial coupling [cf. Eq. (14)] as for the hyperskew interface orientation [cf. Eq. (10)], thus, avoiding APF.

Next, consider the d dependence of the boundaries of the regime of 2PC. As noted above, there is a direct correspondence between $p_{eq}(111\cdots) = p_e$ (the upper boundary) in KMC analysis and MF-type treatments. However, due to APF, $p_{eq}(100\cdots)$ in MF-type treatments does not correspond to the lower boundary p_f of the 2PC regime (as it does in KMC analysis). We claim that p_f can be estimated in MF-type treatments from the stationary point for near-vertical interfaces with rare hyperskew steps, i.e., $p_f = \lim_{S\to\infty} p_{eq}(1000\cdots HS)$ as such steps eliminate APF. Support for this claim comes from

TABLE IV. KMC and pair estimates of p_e and p_f and small errors $\delta p_{e(f)} = p_{e(f)}(\text{pair}) - p_{e(f)}(\text{KMC})$.

	KMC p_e	Pair p_e	δp_e	KMC p_f	Pair p_f	δp_f
$d=2$	0.094 40	0.108 31	0.0139	0.0871	0.1056	0.0185
$d=3$	0.139 39	0.142 95	0.0036	0.1353	0.1399	0.0046
$d=4$	0.158 28	0.160 14	0.0019	0.1548	0.1572	0.0024
$d=5$	0.169 14	0.170 42	0.0013	0.1664	0.1679	0.0015

the results in Table IV. The behavior $p_{e(f)} \sim 0.211\,3765 + c_{e(f)}/d$ as $d \to \infty$, as determined from KMC analysis, is confirmed from the MF-type analysis where the $1/d$ scaling is seen as a natural consequence of the form of the spatial coupling. As an aside, this strategy allows comparison of KMC and MF dRDE results for other orientations [25].

VII. CONCLUSIONS

Our analysis indicates shrinking of the width $\Delta p_{eq}(d) \approx 0.014/d$ of the regime of generic 2PC associated with the discontinuous transition in our QCP version of Schloegl's second model on a hypercubic lattice with increasing dimension d. Appropriate application of MF-type dRDEs is shown to be effective in elucidating this behavior particularly the scaling with d. These features and the utility of the dRDE analysis are expected to be general for nonequilibrium reaction models displaying discontinuous transitions. One could extend this analysis to consider nucleation of the more stable phase from the less stable one just outside the 2PC region. The orientation dependence of interface propagation will be reflected in the shapes of evolving droplets [10,11], a feature which again can be elucidated by a MF-type dRDE analysis.

A significant feature of the MF-type dRDE treatment is the appearance of APF. APF is artificial in the sense that it does not occur in the stochastic lattice-gas model due to fluctuations at the interface. Propagation failure in dRDEs of interest is in its own right [26–28]. Papers often identify a critical value in spatial coupling below which there exists propagation failure, behavior which is amplified upon further reducing this coupling [28]. These observations are consistent with our results, e.g., amplified APF for increasing d.

ACKNOWLEDGMENTS

This work was supported by the U.S. Department of Energy (USDOE), Basic Energy Sciences, Division of Chemical Sciences, Geosciences, and Biosciences, through the Ames Laboratory Chemical Physics and PCTC projects. The Ames Laboratory is operated for the USDOE by Iowa State University under Contract No. DE-AC02-07CH11358.

APPENDIX A: PAIR dRDES

The pair approximation is applied to Eqs. (1) and (3) for spatially inhomogeneous states corresponding to planar interfaces between active and vacuum states. For planar interfaces with a hyperskew $(1111\cdots)$ orientation so that $C_{i1,i2,\ldots,id} = C_{i1+i2+\cdots+id} = C_m$, we let $\varepsilon_m = 1 - C_m$ denote the probability that a site on the hyperskew plane $m = i_1 + i_2 + \cdots + i_d$ is empty. The probability of a NN empty pair with one site in plane m and the other in plane $m+1$ is denoted by $\phi_{m+1/2}$. Then, the corresponding dRDEs have the form

$$d/dt\,\varepsilon_m = p(1-\varepsilon_m) - (2\varepsilon_m - \phi_{m+1/2} - \phi_{m-1/2})^2/(4\varepsilon_m), \tag{A1a}$$

$$\begin{aligned} d/dt\,\phi_{m-1/2} = {} & p(\varepsilon_m + \varepsilon_{m-1} - 2\phi_{m-1/2}) - \phi_{m-1/2} \\ & \times [d(\varepsilon_m - \phi_{m+1/2})^2 + 2(d-1) \\ & \times (\varepsilon_m - \phi_{m+1/2})(\varepsilon_m - \phi_{m-1/2}) \\ & + (d-2)(\varepsilon_m - \phi_{m-1/2})^2]/[4d(\varepsilon_m)^2] \\ & - \phi_{m-1/2}[d(\varepsilon_{m-1} - \phi_{m-3/2})^2 \\ & + 2(d-1)(\varepsilon_{m-1} - \phi_{m-3/2})(\varepsilon_m - \phi_{m-1/2}) \\ & + (d-2)(\varepsilon_m - \phi_{m-1/2})^2]/[4d(\varepsilon_{m-1})^2]. \end{aligned} \tag{A1b}$$

These pair dRDEs reduce to those of the MF dRDEs in the limit as $d \to \infty$.

For a vertical $(1000\cdots)$ interface where $C_{i1,i2,\ldots,id} = C_{i1} = C_m$, we let $\varepsilon_m = 1 - C_m$. The probability of a NN empty pair with one site in plane m and the other in plane $m+1$ [i.e., sites $(i_1, i_2, \ldots, i_d)$ and $(i_1+1, i_2, \ldots, i_d)$] is denoted by $\phi_{m+1/2}$. In addition, we must consider the distinct probability ψ_m of the NN empty pair with both sites in plane m. The corresponding dRDEs have the form

$$\begin{aligned} d/dt\,\varepsilon_m = {} & p[1-\varepsilon_m] - [\varepsilon_m - \psi_m][d\varepsilon_m \\ & - (d-2)\psi_m - \phi_{m+1/2} - \phi_{m-1/2}]/[d\varepsilon_m], \end{aligned} \tag{A2a}$$

$$\begin{aligned} d/dt\,\phi_{m-1/2} = {} & p[\varepsilon_m + \varepsilon_{m-1} - 2\phi_{m-1/2}] - \phi_{m-1/2}[\varepsilon_m - \psi_m] \\ & \times [(d-1)\varepsilon_m - (d-2)\psi_m - \phi_{m+1/2}]/[d(\varepsilon_m)^2] \\ & - \phi_{m-1/2}[\varepsilon_{m-1} - \psi_{m-1}][(d-1)\varepsilon_{m-1} \\ & - (d-2)\psi_{m-1} - \phi_{m-3/2}]/[d(\varepsilon_{m-1})^2], \end{aligned} \tag{A2b}$$

$$\begin{aligned} d/dt\,\psi_m = {} & 2p[\varepsilon_m - \psi_m] - \psi_m[\varepsilon_m - \psi_m][2(d-1)^2\varepsilon_m \\ & - 2(d-2)^2\psi_m - (2d-3)(\phi_{m+1/2} \\ & + \phi_{m-1/2})]/[d(d-1)(\varepsilon_m)^2]. \end{aligned} \tag{A2c}$$

Examination of the form of Eqs. (A2) reveals that the active state cannot displace the vacuum state, consistent with exact behavior in the stochastic model.

APPENDIX B: dRDE PERTURBATION ANALYSIS FOR VERTICAL INTERFACES AS $d \to \infty$

For a stationary planar vertical interface between the vacuum state on the left for $m = 0, -1, -2, \ldots$, and a populated state on the right for $m = 1, 2, \ldots$, the MF dRDE (11) implies that

$$p - C_m(1-C_m) = d^{-1}(1-C_m)(C_{m+1} - 2C_m + C_{m-1}) \quad \text{for } m \geqslant 1, \tag{B1}$$

where $C_0 = 0$. For large d, the RHS is small which forces $p - C_m(1-C_m) \approx 0$ or $C_m \approx C_{\text{act}}$. Thus, it is natural to write $C_m = C_{\text{act}} - \delta_m$ for $m \geqslant 1$ where $\delta_m \ll 1$ from which one

TABLE V. Behavior of δ_m versus m and versus d from a MF dRDE analysis for vertical interfaces at $p = p_{eq}$.

d	δ_1	δ_2	δ_3	δ_4	δ_5	δ_6	δ_6
10	0.1687	2.02×10^{-2}	22.0×10^{-4}	2.39×10^{-4}	2.58×10^{-5}	2.78×10^{-6}	3.01×10^{-7}
100	0.0504	2.25×10^{-3}	9.79×10^{-5}	4.26×10^{-6}	1.85×10^{-7}		
1000	0.0161	2.44×10^{-4}	3.69×10^{-6}	5.57×10^{-8}			
10 000	0.0077	3.56×10^{-5}	1.67×10^{-7}				

obtains

$$(2C_{\rm act}-1)\delta_1 - d^{-1}C_{\rm act}(1-C_{\rm act}) - (\delta_1)^2 - d^{-1}(2-3C_{\rm act}) \times \delta_1 - d^{-1}(1-C_{\rm act})\delta_2 - d^{-1}\delta_1(\delta_2 - 2\delta_1) = 0, \quad \text{(B2a)}$$

$$(2C_{\rm act}-1)\delta_m - d^{-1}(1-C_{\rm act})(\delta_{m+1} - 2\delta_m + \delta_{m-1}) - (\delta_m)^2 - d^{-1}\delta_m(\delta_{m+1} - 2\delta_m + \delta_{m-1}) = 0 \quad \text{for} \quad m > 1. \quad \text{(B2b)}$$

First, we consider the general case of a stationary interface for fixed $p < p_{eq}(d)$ where $2C_{\rm act} - 1 = (1-4p)^{1/2} = O(1)$. It follows from Eq. (B2a) where the first two terms dominate that $d_1 \approx d^{-1}C_{\rm act}(1-C_{\rm act})(2C_{\rm act}-1)^{-1} = O(d^{-1})$. Then, considering the first two dominant terms in Eq. (B2b) implies that $d_m \approx d^{-1}(1-C_{\rm act})(2C_{\rm act}-1)^{-1}d_{m-1}$, which, in turn, yields

$$\delta_m \approx C_{\rm act}(1-C_{\rm act})^m(2C_{\rm act}-1)^{-m}d^{-m} \quad \text{for} \quad m \geqslant 1. \quad \text{(B3)}$$

Second, in the special case of a stationary interface for $p = p_{eq}(d)$, one might anticipate distinct scaling behavior in the situation where $p_{eq}(d) \to \frac{1}{4}$ as $d \to \infty$. Indeed, analysis of numerical data in Table II indicates that $\frac{1}{4} - p_{eq}(d) \approx A/d$ where $A \approx 0.25$ so that $2C_{\rm act} - 1 = (1-4p)^{1/2} \approx B/d^{1/2}$ where $B \approx 1.0$. This forces modified scaling from Eqs. (B2) above. Now, the first three terms in Eq. (B2a) dominate, and one concludes that $B \geqslant 1$ and $\delta_1 \approx E/d^{1/2}$ where $E = \frac{1}{2}[B \pm (B^2-1)^{1/2}]$. Then, considering the first two dominant terms in Eq. (B2b) imply that $d_m \approx \frac{1}{2}d^{-1/2}B^{-1}d_{m-1}$ for $m > 1$, which, in turn, yields

$$\delta_m \approx (2B)^{-m+1}Ed^{-m/2} \quad \text{for} \quad m \geqslant 1. \quad \text{(B4)}$$

Data from numerical analysis of the MF dRDEs support this analysis. See Table V.

[1] J. Marro and R. Dickman, *Nonequilibrium Phase Transitions in Lattice Models* (Cambridge University Press, Cambridge, UK, 1999).

[2] G. Odor, Rev. Mod. Phys. **76**, 663 (2004).

[3] J. Cardy, *Scaling and Renormalization in Statistical Physics* (Cambridge University Press, Cambridge, UK, 1996).

[4] F. Schloegl, Z. Phys. **253**, 147 (1972).

[5] P. Grassberger, Z. Phys. B: Condens. Matter **47**, 365 (1982).

[6] J. P. Boon, D. Dab, R. Kapral, and A. Lawniczak, Phys. Rep. **273**, 55 (1996).

[7] S. Prakash and G. Nicolis, J. Stat. Phys. **86**, 1289 (1997).

[8] R. Durrett, SIAM Rev. **41**, 677 (1999).

[9] D.-J. Liu, X. Guo, and J. W. Evans, Phys. Rev. Lett. **98**, 050601 (2007).

[10] X. Guo, J. W. Evans, and D.-J. Liu, Physica A **387**, 177 (2008). Sites in the last two loss terms in Eq. (B1) are mislabeled. One should replace i with $i - 1$.

[11] X. Guo, D.-J. Liu, and J. W. Evans, J. Chem. Phys. **130**, 074106 (2009).

[12] X. Guo, Y. de Decker, and J. W. Evans, Phys. Rev. E **82**, 021121 (2010).

[13] C.-J. Wang, X. Guo, D.-J. Liu, and J. W. Evans, J. Stat. Phys. **144**, 1308 (2011).

[14] A. L. Toom, in *Multicomponent Random Systems*, edited by R. L. Dobrushin and Y. G. Sinai (Dekker, New York, 1980).

[15] C. H. Bennett and G. Grinstein, Phys. Rev. Lett. **55**, 657 (1985).

[16] R. S. MacKay, Nonlinearity **21**, T273 (2008).

[17] For systems with finite linear size L, an alternative criterion is to balance rates for transitions between states due to homogeneous fluctuations. See G. Nicolis and J. W. Turner, Ann. N.Y. Acad. Sci. **316**, 251 (1979); J. Ross, K. L. C. Hunt, and M. O. Vlad, J. Phys. Chem. C **106**, 10951 (2002). Only for $L \gg L_c$ (characteristic interface width) does this criterion match stationary interfaces.

[18] R. M. Ziff, E. Gulari, and Y. Barshad, Phys. Rev. Lett. **56**, 2553 (1986).

[19] P. Fischer and U. M. Titulaer, Surf. Sci. **221**, 409 (1989).

[20] J. W. Evans and T. R. Ray, Phys. Rev. E **50**, 4302 (1994).

[21] R. H. Goodman, D. S. Graff, L. M. Sander, P. Leroux-Hugon, and E. Clément, Phys. Rev. E **52**, 5904 (1995).

[22] Y. De Decker, G. A. Tsekouras, A. Provata, T. Erneux, and G. Nicolis, Phys. Rev. E **69**, 036203 (2004).

[23] R. M. Ziff and B. J. Brosilow, Phys. Rev. A **46**, 4630 (1992).

[24] J. W. Evans, Rev. Mod. Phys. **65**, 1281 (1993).

[25] KMC estimates for $p_{eq}(110\cdots)$ of 0.1390, 0.1576, and 0.1682 compare with pair estimates of 0.1425, 0.1594, and 0.1694 for $d = 3$–5, respectively. KMC estimates for $p_{eq}(1110\cdots)$ of 0.1581 and 0.1688 compare with pair estimates of 0.1599 and 0.1700 for $d = 4$ and 5, respectively.

[26] J. P. Keener, SIAM J. Appl. Math. **47**, 556 (1987).

[27] S.-N. Chow, J. Mallet-Paret, and E. S. Van Vleck, Int. J. Bifurcation Chaos **6**, 1605 (1996).

[28] G. Fath, Physica D **116**, 176 (1998).